


High Average Gradient in a Laser-Gated Multistage Plasma Wakefield AcceleratorA. Knetsch^{1,*}, I. A. Andriyash¹, M. Gilljohann¹, O. Kononenko¹, A. Matheron¹, Y. Mankovska¹,
P. San Miguel Claveria¹, V. Zakharova¹, E. Adli², and S. Corde¹¹*LOA, ENSTA Paris, CNRS, Ecole Polytechnique, Institut Polytechnique de Paris, 91762 Palaiseau, France*²*Department of Physics, University of Oslo, N-0316 Oslo, Norway* (Received 5 October 2022; revised 27 April 2023; accepted 23 August 2023; published 27 September 2023)

Plasma wakefield accelerators driven by particle beams are capable of providing accelerating gradient several orders of magnitude higher than currently used radio-frequency technology, which could reduce the length of particle accelerators, with drastic influence on the development of future colliders at TeV energies and the minimization of x-ray free-electron lasers. Since interplasma components and distances are among the biggest contributors to the total accelerator length, the design of staged plasma accelerators is one of the most important outstanding questions in order to render this technology instrumental. Here, we present a novel concept to optimize interplasma distances in a staged beam-driven plasma accelerator by drive-beam coupling in the temporal domain and gating the accelerator via a femtosecond ionization laser.

DOI: [10.1103/PhysRevLett.131.135001](https://doi.org/10.1103/PhysRevLett.131.135001)

Electron particle accelerators regularly demonstrate great utility to a variety of scientific disciplines, such as in the form of x-ray free-electron lasers for photon science and their applications or colliders for particle physics. Limited by the accelerating field of state-of-the-art accelerator modules, free-electron lasers driven by linear accelerators (linacs) already span several kilometers in length. To meet the requirements of future electron-positron colliders, conventional linac-based machines with center-of-mass energies beyond 250 GeV and up to several TeV, will reach tens of kilometers in length. Here, plasma wakefield accelerators (PWFAs) offer a promising alternative to the trend of ever-growing particle accelerators. Dense beams of relativistic charged particles can excite plasma wakes with accelerating gradients of 10–100 GV/m [1], in which a trailing electron beam can gain energy on much shorter distances. With such high fields inside the plasma accelerator, the resulting length of a linac becomes defined not as much by the size of the accelerator stage anymore, but rather by the general configuration of the machine. Therefore, a better figure of merit is the average accelerating gradient E_{avg} , which is the ratio between the mean energy gained by a particle beam and the total length of the accelerator. For example, for the future international linear collider (ILC) based on conventional linac technology, this value estimates as $E_{\text{avg}}^{\text{ILC}} = 31.5$ MV/m for the overall length of 30–50 km [2]. There is no consensus yet on how large E_{avg} would be in the case of a PWFA collider facility, but the value should be close to 1 GV/m to be competitive.

In PWFAs, the energy from a drive beam is transferred to a trailing beam, such that an auxiliary preaccelerator as a source of the driver is required. If the trailing beam and

drive beams arrive at similar energies at a PWFA, the trailing-beam energy can be doubled in a single plasma accelerator stage, as demonstrated in the seminal work by Blumfeld *et al.*, in which the tail of a beam was accelerated in the wake, driven by its head [3]. These results motivate the concept of a PWFA afterburner, i.e., a plasma stage that can be added at the end of an accelerator as an energy-doubling device. However, even in such a desirable constellation, the total length of the accelerator still remains tens-of-km scale, and the average gradient is only improved by a factor of approximately 2. Using multiple stages offers a more elegant solution [4]. If a series of beams with much lower energy than the final trailing-beam energy is applied to transfer energy to the trailing beam in consecutive stages, the preaccelerator delivering the drive beams can be kept short and E_{avg} can be much higher [4]. Of course, this scheme comes with its own challenges. Interplasma components for in-coupling and out-coupling of drive beams and transport of trailing beams between stages exceed the length of the plasma in most designs, strongly reduce E_{avg} , and may degrade emittance [5]. Maintaining a high average accelerating gradient throughout the accelerator is therefore a major challenge of staging in PWFA when applied to TeV colliders [6,7]. Staging has been identified by several roadmap publications as a critical development step for advanced particle accelerators [8–10]. Even an electron-only solution might already be of great value for $e^+ e^-$ colliders [11]. Nevertheless, staging of PWFAs was not tested experimentally, so far. A first demonstration of two consecutive laser-driven plasma accelerators [12] showed the feasibility of the concept, however, at few-percent charge coupling efficiency, which emphasizes the significance of the beam-transport design.

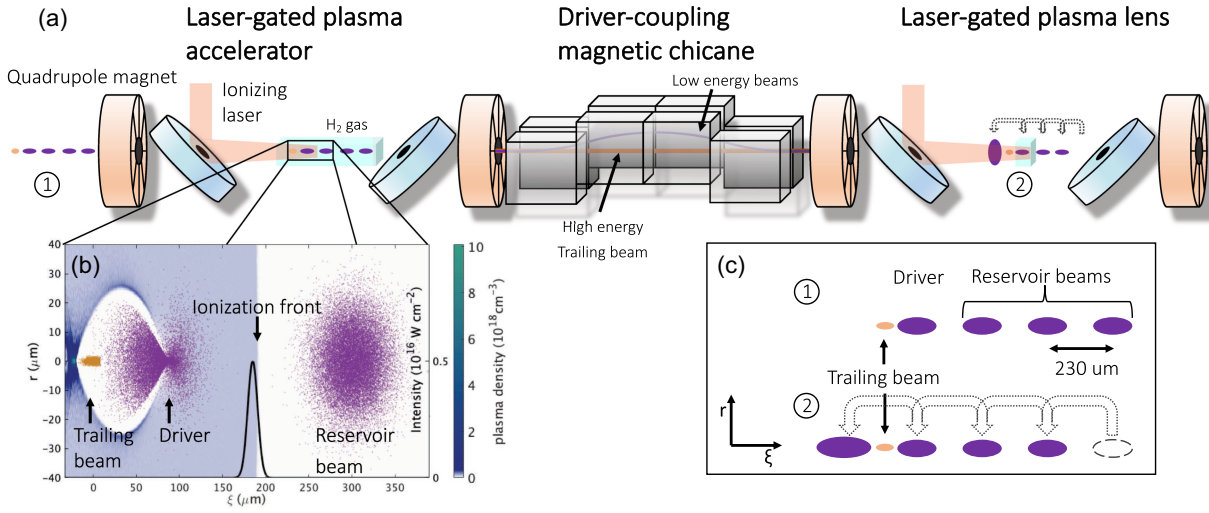


FIG. 1. Sketch of acceleration stage (a) showing a PWFA, a chicane section to extract and insert new driver beams from the beam reservoir and a plasma lens to refocus the trailing beam onto the subsequent PWFA. The concept of laser gating is illustrated by a PIC snapshot, showing reservoir beam, drive beam, trailing beam, and a central cut through the plasma density. (b). The intensity of the fully resolved ionization laser is plotted in black. A sketch of the bunch-train configuration before the PWFA and after the subsequent chicane is shown in (c).

Here, we suggest a staging method that reduces the footprint of interstage beamline components and thereby presents a scalable concept with high average accelerating gradient. Instead of using parallel beamlines for drive and trailing beams [13], we propose to transport all beams on the same axis and perform in-coupling and out-coupling of drive beams in the temporal domain. This is possible because of a unique feature of laser-ionized PWFAs—the ultrashort ionization front of femtosecond laser pulses.

The concept is illustrated in Fig. 1 and builds on three types of beams that propagate in one bunch train, but follow different orbits. The previously introduced *driver* and *trailing* beam that interact in either a PWFA or a plasma lens, and beams that are not yet participating in a plasma accelerator, which we will call *reservoir* beams. The reservoir beams form a bunch train with a small longitudinal spacing (here $\Delta\xi_{\text{res}} = 230 \mu\text{m}$) in the comoving coordinate $\xi = z - ct$, (c being the vacuum speed of light) and are transported by quadrupoles with alternating sign of magnetic field (a so-called focusing-defocusing or FODO lattice). Subsequent to the reservoir-bunch train follows the drive beam and finally the trailing beam. Bunch trains with small spacing and few pC of charge have been demonstrated before [14] and are considered to resonantly excite PWFAs [15]. To increase the charge of bunch trains to 100s of pC, e.g., velocity bunching [16] or collimators in dispersive sections [17] could be promising methods. After every plasma stage, a driver was used up and the trailing beam either gained energy or was refocused in a plasma lens [18]. Depending on the trailing-beam energy, the plasma density and the length of the plasma, a beam-driven wakefield of a plasma stage acts predominantly as an accelerator or a lens. The focusing constituents of the

wakefield in a dense and long PWFA can guide the trailing beam through many transverse betatron oscillations during the acceleration process, while the plasma lens is kept short and thin such that the trailing beam performs much less than one envelope oscillation and thus is focusing. Furthermore, the strong focusing fields in the plasma lens scales linearly with the radial distance from the center of the beam, which is advantageous to avoid emittance growth. As shown in a particle-in-cell (PIC) simulation snapshot in Fig. 1(b), the proposed spacing pattern is wide enough to fit a typical laser pulse from a titanium-sapphire laser system with central wavelength of 800 nm and a pulse length of 23 fs focused down to a spot size of $w_0 = 100 \mu\text{m}$ between electron beams. The laser pulse with a peak intensity of $I_0 = 5 \times 10^{15} \text{ Wcm}^{-2}$ fully ionizes hydrogen gas and the short ionization front gates-out reservoir beams that propagate in gas from driver and trailing beam that interact in a plasma wake. To ionize a plasma channel spanning tens of centimeters, axicon lenses have proven to be a successful optic in previous PWFA experiments [19]. Synchronization requirements between lasers and electron beams from linacs are well within state-of-the-art capabilities. Timing jitters of only a few tens of femtoseconds were demonstrated in free electron laser facilities [20]. Every second FODO half-cell includes a chicane that delays all reservoir beams and that way couples out the depleted driver to the back of the trailing beam. Simultaneously, a fresh reservoir beam becomes a new driver for the subsequent plasma stage. An important advantage of this scheme, when compared to off-axis coupling strategies [4,13], is that the trailing beam by design does not accumulate dispersion from the dipoles, which could otherwise increase its emittance. While magnetic chicanes have been suggested

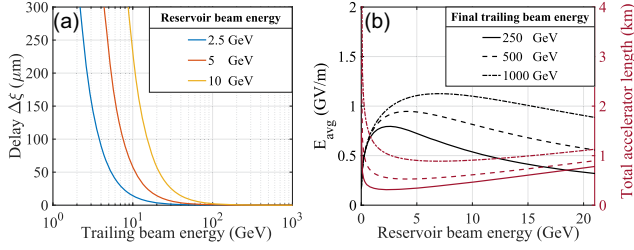


FIG. 2. Trailing-beam delay accumulated in a chicane as a function of energy for different chicane designs, where the reservoir-beam delay is always kept at 230 μm (a). Total length (red) and corresponding average gradient (black) of a staged laser-gated PWFA accelerator, depending on reservoir-beam energy and final trailing-beam energy are plotted in (b).

before in the context of staged plasma accelerators with the aim to regulate energy spread of the trailing beams [21–23], we suggest here chicanes that leave the trailing beam mostly unperturbed.

To generate the desired delay, we propose to use a simple symmetric C chicane consisting of four identical dipoles with magnetic field B_D and a dipole length of L_D in which electron beams move at relativistic velocity, expressed by their Lorentz factor γ . Owing to the longer path length of electrons in a chicane, the beams exit the chicane with a delay expressed in ξ . To minimize the chicane length, we assume no drift between dipoles such that the delay that a particle accumulates per chicane is

$$\Delta\xi = 4L_D \left[\sin^{-1} \left(\frac{L_D}{R_{\text{gyr}}} \right) \frac{R_{\text{gyr}}}{L_D} - 1 \right], \quad (1)$$

where $R_{\text{gyr}} = (\gamma m_e c / q_e B_D)$ is the gyration radius for electrons with mass m_e and charge q_e inside the magnetic field.

The trailing beam needs to be at higher energy than the reservoir beams to remain unaffected by the chicanes. This requirement is explored quantitatively in Fig. 2(a), where Eq. (1) is evaluated for different chicane parameters and trailing-beam energies. E.g., in chicanes that delay reservoir beams with an energy of 10 GeV by $\Delta\xi_{\text{res}}$, a trailing beam at 100 GeV accumulates a delay of $\approx 2.2 \mu\text{m}$. Considering a plasma density of 10^{17} cm^{-3} with a plasma wavelength of 106 μm , this is equivalent to a phase offset of $\approx 1.2^\circ$ and can easily be compensated for by fine adjusting chicane parameters. In the important energy range of 0.1–1 TeV, trailing-beam delays in ξ converge toward 0. Here, chicanes can effectively be built self-similar. As a next step, reservoir-beam energies are optimized to maximize E_{avg} by calculating the total length of the accelerator,

$$L_{\text{acc}} = \frac{4L_{\text{chicane}} W_{\text{final}}}{T W_{\text{driver}}} + \frac{W_{\text{driver}}}{E_{\text{avg,pre}}}. \quad (2)$$

The length of one repeating stage is at least 4 times the chicane length L_{chicane} . Then, the number of stages required to reach the desired final trailing-beam energy W_{final} depends on the fraction of the drive-beam energy W_{driver} that the trailing beam gains in one PWFA stage $T = (\Delta W_{\text{tra}} / W_{\text{driver}})$. We assume $T = 1.5$ as justified by PIC simulations. For simplification, we neglect the length of a final focusing section of a collider or undulator sections in case of an free electron laser. The second term describes the length of the preaccelerator. Here, we use $E_{\text{avg,pre}} = E_{\text{avg}}^{\text{ILC}}$, which could be increased, e.g., by applying x-band cavities [24]. Equation (2) is plotted in Fig. 2(b) and demonstrates that optimal conditions vary, depending on the target energy. The calculations for Fig. 2(b) are performed for dipoles with a magnetic field of 1.5 T. At this value, superconducting magnets are not necessary, since permanent dipoles in Halbach-like configuration can reach magnetic strengths of $> 2 \text{ T}$ [25]. The results based on these simple scaling laws indicate that an accelerator consisting of laser-gated PWFAs could exceed an average gradient of 1 GV/m.

To demonstrate the concept, a system of two consecutive PWFAs and one plasma lens was numerically modeled from start to end for a 100 GeV trailing beam, i.e., equivalent to 12 preceding plasma stages. Figure 3 illustrates the transport of the different beam types. Reservoir beams with an energy of 10 GeV and a charge of 700 pC follow only the magnetic lattice. The quadrupole magnets with a magnetic field strength of 146 T/m and a length of 10 cm are placed at an edge-to-edge distance of 2.2 m. Chicanes consist of four 0.55 m long dipoles with a magnetic field of 1.27 T after a PWFA and 1.73 T after a plasma lens (corresponding to a delay of 160 μm and 300 μm respectively). This pattern sets a distance of $\Delta\xi_{\text{tra}} \approx 70 \mu\text{m}$ between driver and trailing beam in the PWFA

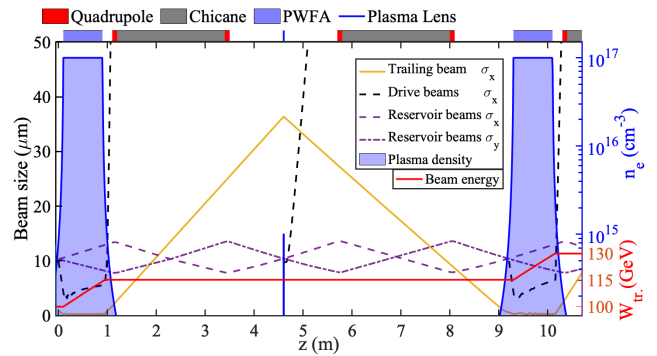


FIG. 3. Transport of different beam types between plasma stages. Reservoir beams propagate in a FODO lattice and are not influenced by plasma wakes, as they arrive too early. Drive beams lose energy to the plasma wake and leave the plasma with increased divergence. The trailing beam is refocused by a plasma lens (thin blue area) between the PWFA stages (wide blue area). Mean trailing-beam energy gain is plotted as red line.

stages and $\approx 140 \mu\text{m}$ in the plasma lens stages. The larger spacing has the advantage, that the wake inside the plasma lens is widened at the location of the trailing beam and full charge collection is ensured. After the very first PWFA stage, the trailing beam is accelerated from 10 GeV to approximately 25 GeV. Here, one can apply a magnetic-field pattern of 1.5 T and 1.8 T, corresponding to a driver-trailing spacing of $\approx 70 \mu\text{m}$ in the PWFA and $\approx 111 \mu\text{m}$ in the plasma lens.

The reservoir-beam propagation was simulated with the code ELEGANT [26] in the SIREPO framework [27–30] and optimized such that a drive beam is radially symmetric at the entrance of a plasma with a root-mean-square (rms) spot size of $10 \mu\text{m}$. Coherent synchrotron radiation (CSR) increases the full-width-half-maximum energy spread and rms length of a reservoir bunch from initially 0.24% and $22.0 \mu\text{m}$ to 4.4% and $22.7 \mu\text{m}$ after 12 chicanes. After 44 chicanes, the bunch length is doubled, which impedes a strong plasma wakefield beyond this point. The bunch train itself is not dense enough to ionize hydrogen [31–33]. E.g., integrating the tunnel-ionization rates [32] induced by the self-fields of 100 reservoir beams results in a maximum ionization ratio of just 7.3×10^{-11} . Owing to large energy gains per PWFA stage, CSR and quantum-diffused incoherent synchrotron radiation [34,35] can be expected to have a minor effect on the trailing beam with a per-mille relative-energy-spread contribution after acceleration to 1 TeV.

The three plasma stages are simulated with the quasistatic PIC code HiPACE++ [36,37]. Between stages, PIC-simulated macro particles of trailing and drive beams are transported according to linear beam-propagation matrices and delayed following Eq. (1). The simulations were run on $512 \times 512 \times 4096$ grid points with a resolution of $0.58 \mu\text{m} \times 0.58 \mu\text{m} \times 0.05 \mu\text{m}$. The drive-beam distributions were read in from ELEGANT output. The trailing beam with a charge of 50 pC and an initial energy of 100 GeV has a total bunch length of $4 \mu\text{m}$ and a triangular current shape to decrease the growth of energy spread of 0.12%. The homogeneous part of the PWFA plasma is 0.8 m long with a plasma density of 10^{17}cm^{-3} . At the entrance and exit, matching is facilitated by density ramps that follow the function, $n_e(z) = [1/(1 - z/L_r)^2]$ as suggested by Ref. [38] with a length scale $L_r = 0.01 \text{m}$. The density ramps cannot be arbitrarily long, because the trailing beam slips into the decelerating phase of the wake at low densities and loses energy. Therefore, the trailing beam is being refocused in a plasma lens with a length of $L_{\text{lens}} = 6.5 \text{mm}$ and a plasma density $n_{e,l} = 1 \times 10^{15} \text{cm}^{-3}$. Its focal length roughly follows the theoretical scaling law $f = (2\gamma/k_p^2 L_{\text{lens}}) \propto (\gamma/L_{\text{lens}} n_{e,l}) (k_p^{-1}$ being the plasma skin depth) such that trailing beams are imaged onto the entrance of the subsequent PWFA with a magnification close to 1. One can easily see that f can be kept constant up to a trailing-beam energy of 1 TeV, either by scaling up $n_{e,l}$ or by increasing

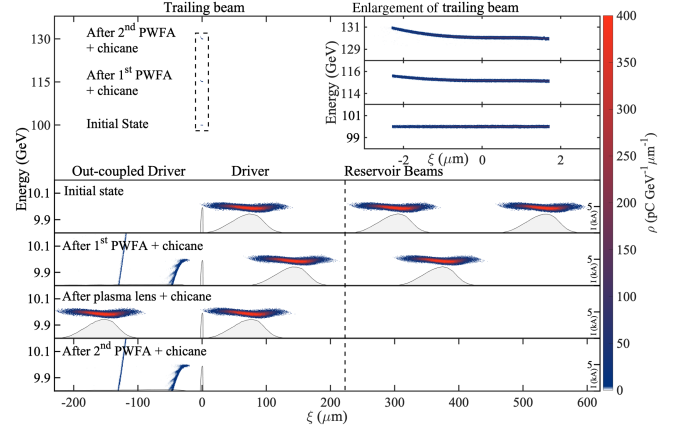


FIG. 4. Numerical modeling of the longitudinal phase space at different locations. Trailing-beam distributions are plotted as initial state, after accelerating sections (top left) and as enlargement (top right). For driver and reservoir beams, macroparticle distributions are plotted combined with the current (bottom). All macroparticles are delayed following Eq. (1).

L_{lens} . Even magnification between stages can be independently fine-tuned. Figure 4 explores the development of the longitudinal phase space for different beam types throughout two PWFA stages and a plasma lens. Inside the PWFA stage, the drive beam loses a large fraction of its energy, with a mean energy loss of 5.5 GeV and electrons decelerated down to an energy of 1.6 GeV. Subsequently, the drivers expand radially due to their wide divergence of 3.0 mrad out of the PWFA and 0.15 mrad out of the plasma lens. All drive-beam electrons (from a PWFA or plasma lens) are delayed to $\xi < 0$ in the subsequent chicane and are, as far as the trailing beam is concerned, out coupled. Simultaneously, the driver is replenished by delaying the reservoir beams. In an actual machine, it would be important to dump all the beams in a controlled way. A possible strategy could be to extract the lower-energy part ($< 9 \text{GeV}$) of the depleted beams at the first dipole after the PWFA. Owing to the large energy spread, the particles would arrive at a beam dump as a wide stripe in the dispersive plane. Remaining high-energy parts as well as drive beams of plasma lenses could continue to be transported in the linac and eventually be dumped in a final beam dump. The longitudinal phase space of the trailing beam is plotted in its initial state and after each simulated PWFA. Over the path of two PWFA stages, the trailing beam gains 30.1 GeV, which confirms $T \approx 1.5$. The achieved values set the average gradient of two accelerator stages to 1.64 GV/m. When considering a preaccelerator with an average gradient of $E_{\text{avg}}^{\text{ILC}}$, a laser-gated PWFA accelerator would span approximately 929 m, and the 102 ps long reservoir-beam train would consist of 133 bunches. Such a machine would provide electron beams with an energy of 1 TeV at a total average gradient of $\approx 1.1 \text{GV/m}$. Reservoir-beam lengthening due to CSR effects might require incoupling of a new reservoir-beam bunch train at every

100 GeV of energy gain. If reserving another 5 m for every septum or similar device, the average gradient would still remain above ≈ 1 GV/m.

In conclusion, the proposed concept of a laser-gated multistage beam-driven plasma accelerator addresses outstanding questions on how a plasma wakefield accelerator can be scaled up to the TeV energy range at a competitive average gradient. By in- and out-coupling the drive beam in the temporal domain and gating the accelerator with femtosecond ionization lasers, this strategy provides a unique opportunity to combine plasma-based and magnet-based lattices on the same axis and thereby reduce the overall accelerator footprint to a few-kilometer scale. Presented results open the way toward compact gamma-gamma [39] and electron-electron [40] colliders, and, by being compatible with laser-ionized beam-driven positron accelerators [41], to $e^+ e^-$ colliders, that are strongly desired for future discoveries in the field of particle and high energy physics.

We acknowledge the Grand Équipement National de Calcul Intensif (GENCI) and Très Grand Centre de Calcul (TGCC) for granting us access to the supercomputer Joliot-Curie on the Irene V100 partition, under Grants No. 2020-A0080510786, No. 2021-A0100510786, No. 2021-A0110510062, No. 2022-A0120510786, and No. 2022-A0130510062, to run PIC simulations. The work was supported by the European Research Council (ERC) under the European Union's Horizon 2020 research and innovation program project Miniature beam-driven Plasma Accelerators (M-PAC), Grant Agreement No. 715807.

*alexander.knetsch@polytechnique.edu

- [1] T. Tajima and J. M. Dawson, *Phys. Rev. Lett.* **43**, 267 (1979).
- [2] The International Linear Collider, edited by T. Behnke, J. E. Brau, B. Foster, J. Fuster, M. Harrison, J. M. Paterson, M. Peskin, M. Stanitzki, N. Walker, and H. Yamamoto, Technical Design Report, [arXiv:1306.6327](https://arxiv.org/abs/1306.6327).
- [3] I. Blumenfeld, C. E. Clayton, F. J. Decker, M. J. Hogan, C. Huang, R. Ischebeck, R. Iverson, C. Joshi, T. Katsouleas, N. Kirby *et al.*, *Nature (London)* **445**, 741 (2007).
- [4] E. Adli, J. Delahaye, S. Gessner, M. Hogan, T. Raubenheimer, W. An, W. Mori, and C. Joshi, *Proceedings of the IPAC13* (JACOW, Geneva, 2013).
- [5] C. A. Lindstrøm and M. Thévenet, *J. Instrum.* **17**, P05016 (2022).
- [6] C. A. Lindstrøm, *Phys. Rev. Accel. Beams* **24**, 014801 (2021).
- [7] B. Cros, P. Muggli, C. Schroeder, S. Hooker, P. Piot, J. England, S. Gessner, J. Vieira, E. Gschwendtner, J.-L. Vay *et al.*, [arXiv:1901.10370](https://arxiv.org/abs/1901.10370).
- [8] F. Albert, M.-E. Couprie, A. D. Debus, M. Downer, J. Faure, A. Flacco, L. A. Gizzi *et al.*, *New J. Phys.* **23**, 031101 (2020).
- [9] R. Assmann, M. Weikum, T. Akhter, D. Alesini, A. Alexandrova, M. Anania, N. Andreev, I. Andriyash, M. Artioli, A. Aschikhin *et al.*, *Eur. Phys. J. Special Topics* **229**, 3675 (2020).
- [10] R. Assmann, E. Gschwendtner, K. Cassou, S. Corde, L. Corner, B. Cros, M. Ferrario, S. Hooker, R. Ischebeck, A. Latina *et al.*, *CERN Yellow Reports* **1**, 91 (2022).
- [11] B. Foster, R. D'Arcy, and C. A. Lindstrøm, [arXiv:2303.10150](https://arxiv.org/abs/2303.10150).
- [12] S. Steinke, J. Van Tilborg, C. Benedetti, C. Geddes, C. Schroeder, J. Daniels, K. Swanson, A. Gonsalves, K. Nakamura, N. Matlis *et al.*, *Nature (London)* **530**, 190 (2016).
- [13] J. Pfungstner, C. A. Lindstrøm, E. Adli, D. Schulte, and E. Marín, in *Proceedings of the International Particle Accelerator Conference* (JACOW, Geneva, 2016).
- [14] E. Kallos, P. Muggli, T. Katsouleas, V. Yakimenko, D. Stolyarov, I. Pogorelsky, I. Pavlishin, K. Kusche, M. Babzien, I. Ben-Zvi *et al.*, in *AIP Conf. Proc.* (American Institute of Physics, College Park, 2006), Vol. 877, pp. 520–526.
- [15] P. Manwani, N. Majernik, M. Yadav, C. Hansel, and J. B. Rosenzweig, *Phys. Rev. Accel. Beams* **24**, 051302 (2021).
- [16] A. Mostacci, D. Alesini, P. Antici, A. Bacci, M. Bellaveglia, R. Boni, M. Castellano, E. Chiadroni, A. Cianchi, G. Di Pirro *et al.*, in *IPAC 2011-2nd International Particle Accelerator Conference* (JACOW, Geneva, 2011), pp. 2877–2881.
- [17] S. Schröder, K. Ludwig, A. Aschikhin, R. D'Arcy, M. Dinter, P. Gonzalez, S. Karstensen, A. Knetsch, V. Libov, C. A. Lindstrøm *et al.*, *J. Phys. Conf. Ser.* **1596**, 012002 (2020).
- [18] C. E. Doss, E. Adli, R. Ariniello, J. Cary, S. Corde, B. Hidding *et al.*, *Phys. Rev. Accel. Beams* **22**, 111001 (2019).
- [19] S. Green, E. Adli, C. Clarke, S. Corde, S. Edstrom, A. Fisher, J. Frederico, J. Frisch, S. Gessner, S. Gilevich *et al.*, *Plasma Phys. Controlled Fusion* **56**, 084011 (2014).
- [20] S. Schulz, I. Grguraš, C. Behrens, H. Bromberger, J. T. Costello, M. K. Czwalińska, M. Felber, M. C. Hoffmann, M. Ilchen, H. Y. Liu *et al.*, *Nat. Commun.* **6**, 5938 (2015).
- [21] A. Ferran Pousa, A. Martinez de la Ossa, R. Brinkmann, and R. W. Assmann, *Phys. Rev. Lett.* **123**, 054801 (2019).
- [22] C. A. Lindstrøm, [arXiv:2104.14460](https://arxiv.org/abs/2104.14460).
- [23] A. Ferran Pousa, I. Agapov, S. A. Antipov, R. W. Assmann, R. Brinkmann, S. Jalas *et al.*, *Phys. Rev. Lett.* **129**, 094801 (2022).
- [24] A. D. Cahill, J. B. Rosenzweig, V. A. Dolgashev, S. G. Tantawi, and S. Weathersby, *Phys. Rev. Accel. Beams* **21**, 102002 (2018).
- [25] M. Kumada, Y. Iwashita, M. Aoki, and E. Sugiyama, in *Proceedings of the 2003 Particle Accelerator Conference* (IEEE, Piscataway, 2003), Vol. 3, pp. 1993–1995.
- [26] M. Borland, Elegant: A flexible SDDS-compliant code for accelerator simulation, Technical Report No. LS-287 TRN: US0004540, Argonne National Lab., IL (US), 2000.
- [27] Sirepo, a community gateway for computer-aided engineering (2023), <https://www.sirepo.com/>.
- [28] Sirepo, an open source framework for cloud computing (2023), <https://github.com/radiasoft/sirepo>.

- [29] J. Edelen, D. Abell, D. Bruhwiler, S. Coleman, N. Cook, A. Diaw, J. Einstein-Curtis, C. Hall, M. Kilpatrick, B. Nash *et al.*, in *5th North American Particle Accelerator Conference (NAPAC'22)* (JACOW Publishing, Geneva, Switzerland, 2022), pp. 164–169.
- [30] D. Bruhwiler, D. Abell, N. Cook, C. Hall, M. Keilman, P. Moeller, R. Nagler, B. Nash *et al.*, in *Proceedings of the International Particle Accelerator Conference* (JACOW, Geneva, 2019).
- [31] M. V. Ammosov, N. B. Delone, and V. Krainov, *Sov. Phys. JETP* **64**, 1191 (1986).
- [32] D. L. Bruhwiler, D. A. Dimitrov, J. R. Cary, E. Esarey, W. Leemans, and R. E. Giacone, *Phys. Plasmas* **10**, 2022 (2003).
- [33] R. Tarkeshian, J. L. Vay, R. Lehe, C. B. Schroeder, E. H. Esarey, T. Feurer, and W. P. Leemans, *Phys. Rev. X* **8**, 021039 (2018).
- [34] N. Yampolsky and B. E. Carlsten, *Nucl. Instrum. Methods Phys. Res., Sect. B* **870**, 156 (2017).
- [35] M. Sands, *Phys. Rev.* **97**, 470 (1955).
- [36] T. Mehrling, C. Benedetti, C. Schroeder, and J. Osterhoff, *Plasma Phys. Controlled Fusion* **56**, 084012 (2014).
- [37] S. Diederichs, C. Benedetti, A. Huebl, R. Lehe, A. Myers, A. Sinn, J.-L. Vay, W. Zhang, and M. Thévenet, *Comput. Phys. Commun.* **278**, 108421 (2022).
- [38] X. L. Xu, J. F. Hua, Y. P. Wu, C. J. Zhang, F. Li, Y. Wan *et al.*, *Phys. Rev. Lett.* **116**, 124801 (2016).
- [39] V. Telnov, *Nucl. Instrum. Methods Phys. Res., Sect. A* **355**, 3 (1995).
- [40] V. Yakimenko, S. Meuren, F. Del Gaudio, C. Baumann, A. Fedotov, F. Fiuza, T. Grismayer, M. J. Hogan, A. Pukhov, L. O. Silva *et al.*, *Phys. Rev. Lett.* **122**, 190404 (2019).
- [41] S. Diederichs, T. J. Mehrling, C. Benedetti, C. B. Schroeder, A. Knetsch, E. Esarey, and J. Osterhoff, *Phys. Rev. Accel. Beams* **22**, 081301 (2019).